Supporting Information

Fractional Recovery of Lignin from Black Liquor Using Acid-Assisted Flocculation with Lignin-Based Flocculants

Shufan Chen [a,#], Fu Su [a,#], Suwan Xing [a], Jianbo Zhao [b], Di Cai [d], Shikun Cheng [e], Marcelo A. Nolasco [f], Nigel J. D. Graham [c], Zhen Yang [a,b*]

[a] School of Chemistry and Materials Science, Jiangsu Provincial Key Laboratory of Material Cycling and Pollution Control, Nanjing Normal University, Nanjing 210023, China

[b] College of Chemistry and Chemical Engineering, Tarim University, Alar 843300, China

[c] Department of Civil and Environmental Engineering, Imperial College London, London, SW7 2AZ, UK

[d] College of Life Science and Technology, National Energy R&D Center for Biorefinery, Beijing University of Chemical Technology, Beijing 100029, China

[e] School of Energy and Environmental Engineering, University of Science and Technology Beijing, Beijing 100024, China

[f] School of Arts, Sciences and Humanities, University of Sao Paulo, Sao Paulo 13635-900, Brazil

[#] Both authors contributed equally.

[*] Corresponding author. E-mail: yangzhen@njnu.edu.cn

Summary

Table. S1. Water quality parameters of black liquor before and after each step of treatment. (S4)

Table. S2. Yield, purity, recovery rate, and other physical-chemical properties of the recovered fractions. (S5)

Table S3. Structural units of lignin in 2D HSQC-NMR. (S6)

Table S4. Raw material price and consumption for L-CTA preparation. (S7)

Fig. S1. Yields (bars) of organic matter with different MWs and purities of the target fraction (MW>5000 Da) (points and curves) using different dosage of $AlCl_3$ (a, c, e, and g) and PAM (b, d, f, and h) at different pHs ((a and b) 13, (c and d) 11, (e and f) 9, and (g and h) 7). (S8)

Fig. S2. (a) Variations of frequency shift (Δf) and dissipation shift (ΔD) as a function of time for the deposition of different lignin fractions on the sensor surface coated with L-CTA; (b) -ΔD/Δf values for different lignin fractions. (S10)

Fig. S3. Raw data of isothermal titration microcalorimeter, as well as the corresponding conversion to heat/molar ratio, at 25 °C, by titrating L-CTA solution into (a) F1, (b) F2 and (c) F3 solutions. (S11)

Fig. S4. Spatial distribution of different substances (10 characteristic fragments of L-CTA and 20 characteristic fragments of lignin (among them, the number of S unit in F1, F2 and F3 is 9, 8 and 7; the number of G unit is 10, 11 and 12; and the number of H unit is 1)) in 100×100×100 Å boxes with 1000 water molecules at 0 and 1000 ps. (S12)

Fig. S5. SEM images of the recovered fractions ((a) F1, (b) F2, and (c) F3). (S13)

Fig. S6. Image analysis for the determination of fractal dimension D_2 of the recovered fractions ((a) F1, (b) F2, and (c) F3). (D_2 was obtained based on the power-law

relationship between projected area and characteristic length of floc particles) (S14)

Fig. S7. Acute toxicity assessment of flocculants using *Daphnia magna* as a model organism: dose–response relationships for (a) L-CTA, (b) lignin, (c) commercial PAM, and (d) AlC_3. The fitted regression lines indicate concentration-dependent toxicity trends. (S15)

Table. S1. Water quality parameters of BL before and after each step of treatment.

	BL	Step 1	Step 2	Step 3
pH	13	7	4	3
Colour (Pt-Co unit)	10574±243	5127±195	589±94	357±51
Lignin (g/L)	35.01±1.34	15.60±0.67	6.55±0.31	3.03±0.27
Total solids (g/L)	66.67±2.76	31.65±1.02	14.34±1.25	8.08±0.76
Organic matter (g/L）	45.10±1.87	23.27±2.03	11.74±0.84	6.20±0.62
Inorganic matter (g/L)	21.87±1.82	8.38±1.01	2.60±0.24	1.88±0.31
COD (mg/L)	3573±103	1715±47	1314±52	982±28
Turbidity (NTU)	2100±137	675±59	297±38	103±29

Table. S2. Yield, purity, recovery rate, and other physical-chemical properties of the recovered fractions.

	F1	F2	F3
Yield (g/L)	19.41±0.64	9.05±0.56	3.52±0.21
Purity (%)	88.87±2.45	78.49±6.04	63.54±9.25
Recovery (%)	91.68±1.45	87.96±2.02	89.46±3.65
C (wt.%)	58.94±0.26	53.12±0.38	46.46±0.53
H (wt.%)	2.61±0.36	3.72±0.26	5.14±0.38
O (wt.%)	17.28±0.35	21.11±0.27	25.36±0.19
N (wt.%)	0.28±0.01	0.62±0.02	1.33±0.01
O/C	0.29±0.03	0.39±0.02	0.54±0.06
VM/FC* (w/w)	1.09±0.10	1.24±0.08	1.44±0.05

* ratio of volatile matter (VM) to fixed carbon (FC)

Table S3. Structural units of lignin in 2D HSQC-NMR.

	δC/δH(ppm)	Assignments
B_β	53.5/3.06	C_β−H_β in resinol substructures (B)
A_γ	59.5-59.7/3.40-3.63	C_γ−H_γ in β-O-4′ substructures (A)
C_γ	62.5/3.73	C_γ−H_γ in phenylcoumaran substructures (C)
A_α	71.8/4.86	C_α−H_α in β-O-4′ substructures (A)
$A_{\beta(G/H)}$	83.9/4.29	C_β−H_β in β-O-4′ substructures linked to G/H units (A)
$A_{\beta(S)}$	85.9/4.12	C_β−H_β in β-O-4′ substructures linked to S units (A)
$S_{2,6}$	103.8/6.71	$C_{2,6}$−$H_{2,6}$ in etherified syringyl units (S)
$S'_{2,6}$	106.2/7.23 and 7.07	$C_{2,6}$−$H_{2,6}$ in oxidized (Cα=O) syringyl units (S′)
G_2	110.9/6.98	C_2−H_2 in guaiacyl units (G)
G_5	114.9/6.77	C_5−H_5 in guaiacyl units (G)
G_6	119.0/6.80	C_6−H_6 in guaiacyl units (G)
$H_{2,6}$	127.9/7.19	$C_{2,6}$−$H_{2,6}$ in p-hydroxyphenyl units (H)
pCA_α	144.8/7.47	C_α−H_α in p-coumarate (*p*CA)
pCA_β	113.7/6.28	C_β−H_β in p-coumarate (*p*CA)
FA_α	144.8/7.47	C_α−H_α in ferulate (FA)
X_2	72.5/3.02	C_2−H_2 in *β*-D-xylopyranoside
X_3	73.7/3.22	C_3−H_3 in *β*-D-xylopyranoside
X_4	75.4/3.60	C_4−H_4 in *β*-D-xylopyranoside

Table S4. Raw material price and consumption for L-CTA preparation.

Material	Price (CNY/g)	Consumption according to the L-CTA preparation process in Section 2.1 (g)
NaOH	2.5×10^{-3} CNY/kg	0.09
CTA	8.0×10^{-3} CNY/kg	2.82
HCl (37 wt.%)	0.1×10^{-3} CNY/kg	2.52

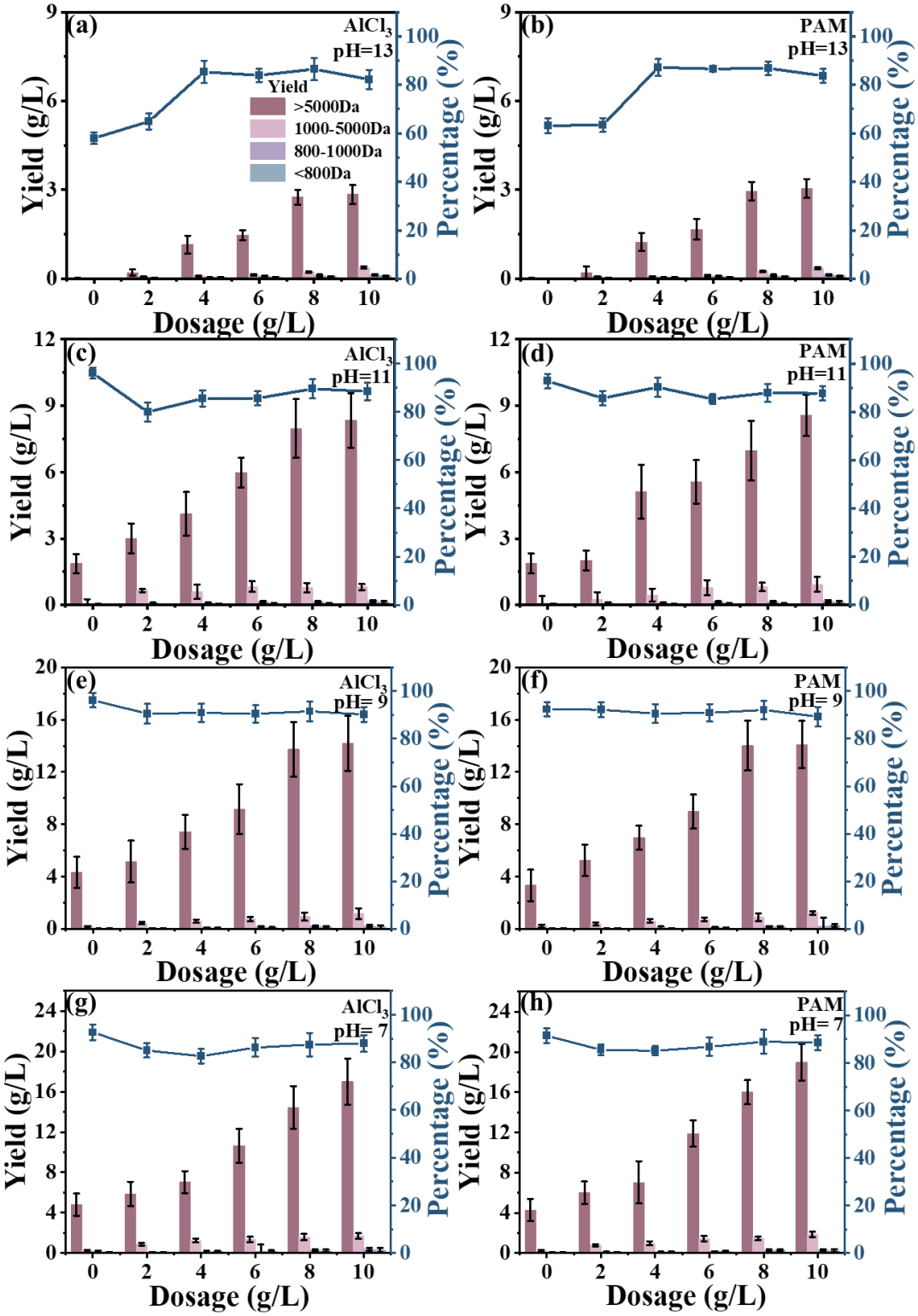


Fig. S1. Yields (bars) of organic matter with different MWs and purities of the target fraction (MW>5000 Da) (points and curves) using different dosages of $AlCl_3$ (a, c, e,

and g) and PAM (b, d, f, and h) at different pHs ((a and b) 13, (c and d) 11, (e and f) 9, and (g and h) 7).

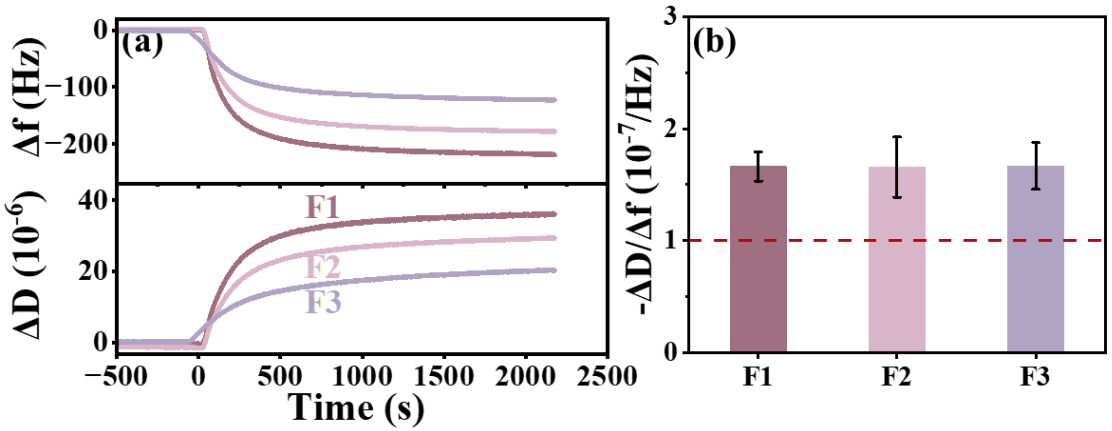


Fig. S2. (a) Variations of frequency shift (Δf) and dissipation shift (ΔD) as a function of time for the deposition of different lignin fractions on the sensor surface coated with L-CTA; (b) -ΔD/Δf values for different lignin fractions.

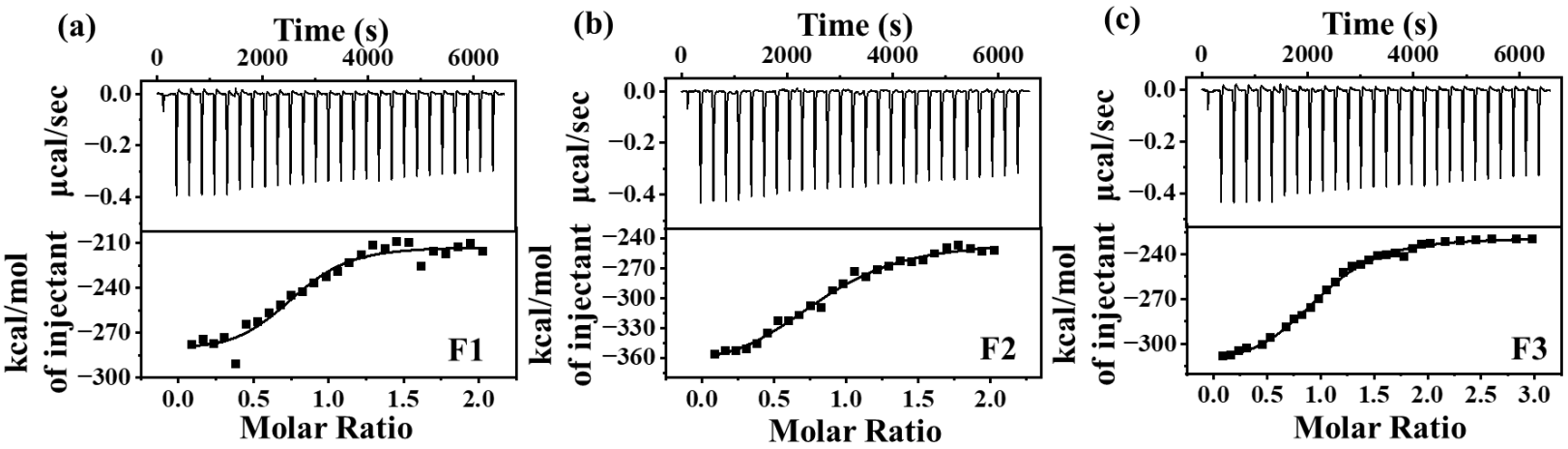


Fig. S3. Raw data of isothermal titration microcalorimeter, as well as the corresponding conversion to heat/molar ratio, at 25 ºC, by titrating L-CTA solution into (a) F1, (b) F2 and (c) F3 solutions.

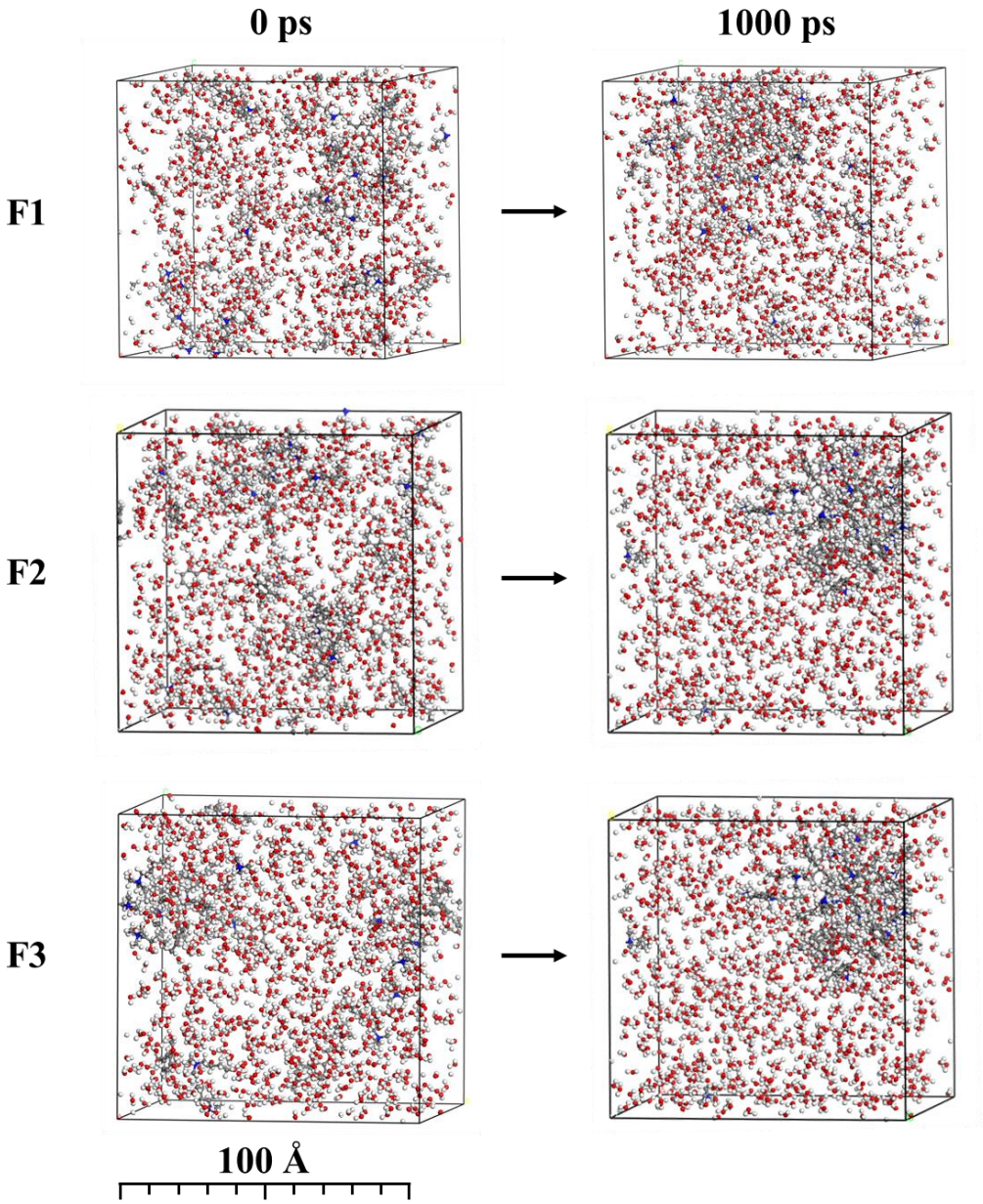


Fig. S4. Spatial distribution of different substances (10 characteristic fragments of L-CTA and 20 characteristic fragments of lignin (among them, the number of S unit in F1, F2 and F3 is 9, 8 and 7; the number of G unit is 10, 11 and 12; and the number of H unit is 1)) in 100×100×100 Å boxes with 1000 water molecules at 0 and 1000 ps.

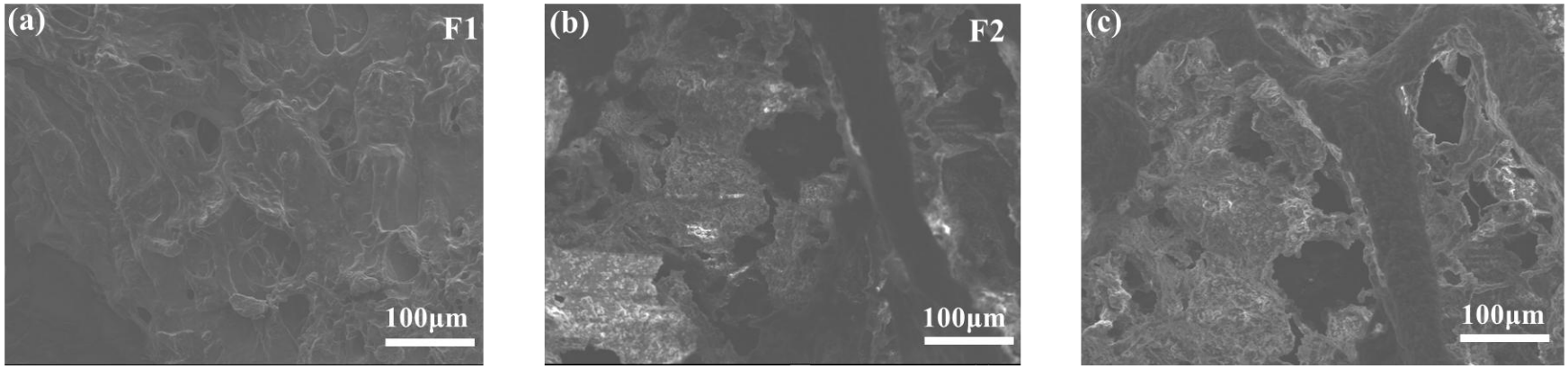


Fig. S5. SEM images of the recovered fractions ((a) F1, (b) F2, and (c) F3).

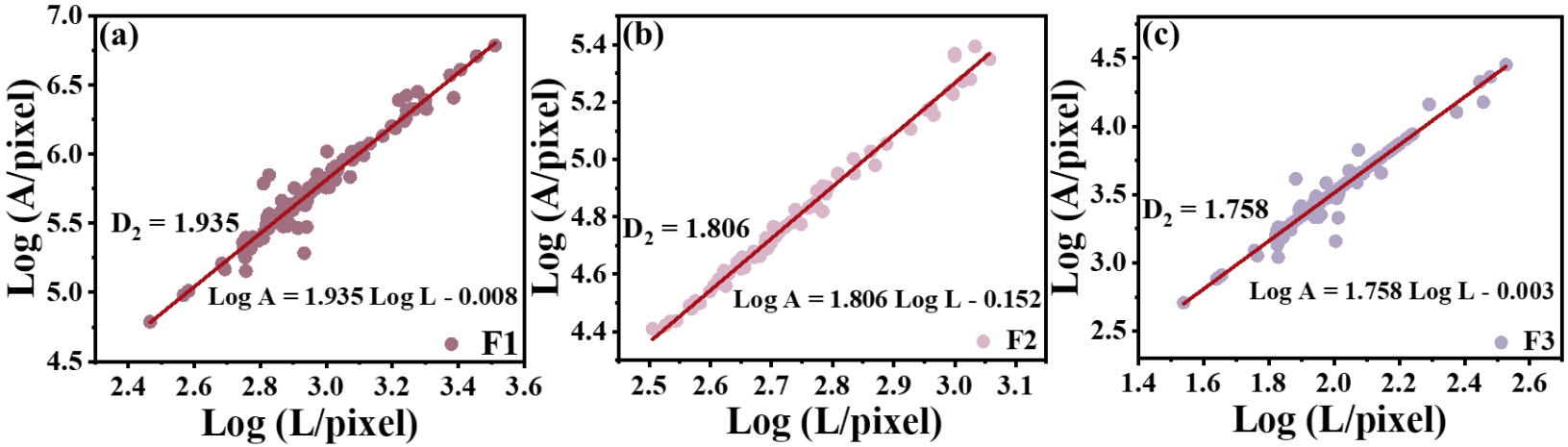


Fig. S6. Image analysis for the determination of fractal dimension D_2 of the recovered fractions ((a) F1, (b) F2, and (c) F3). (D_2 was obtained based on the power-law relationship between projected area and characteristic length of floc particles)

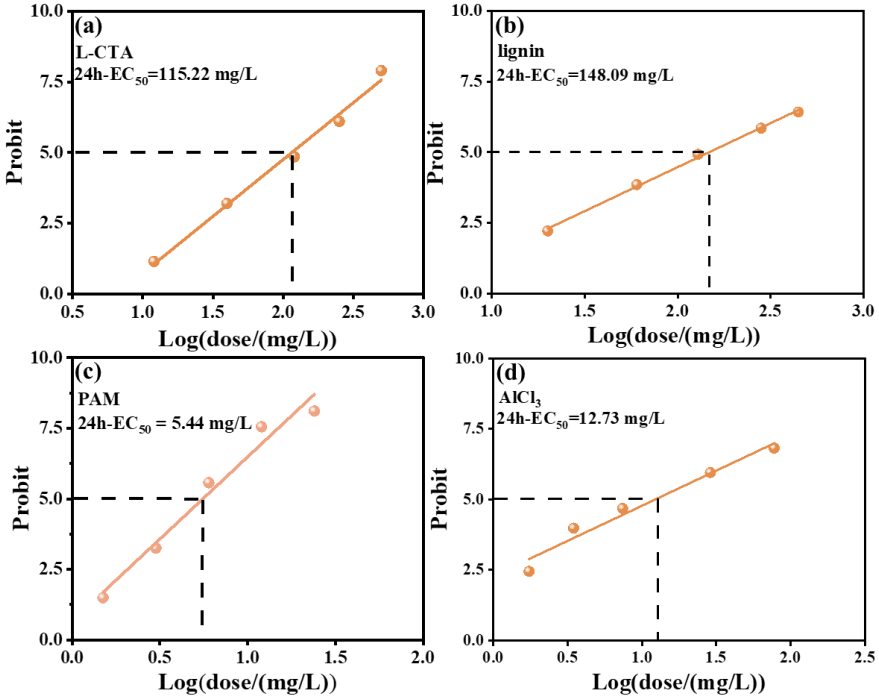


Fig. S7. Acute toxicity assessment of flocculants using *Daphnia magna* as a model organism: dose–response relationships for (a) L-CTA, (b) lignin, (c) commercial PAM, and (d) AlC_3. The fitted regression lines indicate concentration-dependent toxicity trends.